Los Alamos
NATIONAL LABORATORY
EST. 1943

LA-UR-21-27148
Approved for public release; distribution is unlimited.

Title: First principles calculations in support of Pu aging: calculating the effects of lattice imperfections on thermodynamics

Author(s): Rudin, Sven Peter

Intended for: Report

Issued: 2021-07-22

Disclaimer:
Los Alamos National Laboratory, an affirmative action/equal opportunity employer, is operated by Triad National Security, LLC for the National Nuclear Security Administration of U.S. Department of Energy under contract 89233218CNA000001. By approving this article, the publisher recognizes that the U.S. Government retains nonexclusive, royalty-free license to publish or reproduce the published form of this contribution, or to allow others to do so, for U.S. Government purposes. Los Alamos National Laboratory requests that the publisher identify this article as work performed under the auspices of the U.S. Department of Energy. Los Alamos National Laboratory strongly supports academic freedom and a researcher's right to publish; as an institution, however, the Laboratory does not endorse the viewpoint of a publication or guarantee its technical correctness.

First principles calculations in support of Pu aging: calculating the effects of lattice imperfections on thermodynamics

Sven P. Rudin, T-1, LANL

Executive Summary

Plutonium (Pu) has, in theory, well defined crystal structures: its atoms are arranged in regular spatial patterns. But Pu is radioactive, and as its nuclei decay those regular spatial patterns are interrupted. The interruptions are lattice imperfections, which are known to affect how materials respond to their environment. To adequately model Pu, we need to know which lattice imperfections are present, how they interact with each other, and how they affect the material's response to its environment.

The work presented here aims to use density functional theory (DFT) calculations to begin to answer the latter, in particular, how individual lattice imperfections affect measurable effects including thermal expansion (the change in volume in response to a change in temperature), heat capacity (the amount of thermal energy needed to change a material's temperature), and elastic moduli (a material's resistance to applied stresses).

Pu poses many computational challenges. The *f* electrons require special attention. Of all the elements, Pu has the largest number of electrons that must be included in the calculations. Thermal effects require calculating the phonons (the lattice vibrations), which for systems containing lattice imperfections demand large, complex computational cells — but computational resources limit the size and complexity. With careful restructuring of how the calculations are performed, all these challenges have been met to enable calculations that provide insight into how lattice imperfections affect Pu's response to its environment.

Reported here are the computational challenges and the advances developed to meet them, along with the first results showing the strong effect that one prototype lattice imperfection (an interstitial Pu atom in a delta-phase Pu lattice) has on Pu's response to its environment.

Introduction

Phonons contribute critically to determining the thermal properties of crystalline materials. As phonons are the normal modes of vibration of the crystal lattice, the structure of the lattice determines how the forces between the atoms translate into the phonon frequencies and eigenmodes. Consequently, lattice imperfections change the phonons and hence the material's thermal properties. Imperfections such as stacking faults and point defects represent flaws in the periodicity of the material's crystal structure, though their presence can be desirable or undesirable depending on the material's application [Lindsay2019].

The doping of Pu with Ga serves as an example of the former: targeted doping with several atomic percent Ga stabilizes the preferred delta phase into a wider temperature range. However, most of the lattice imperfections in Pu stem from the radioactive decay, and these generally fall into the undesired category. The effect of the plethora of lattice imperfections on Pu's thermal properties has been and continues to be experimentally well studied, but only concomitantly: the effects of individual imperfections is largely unknown.

At the other extreme, DFT calculations cannot be performed with all imperfections present, the required system size is far beyond the approach's feasibility. At best, a few imperfections can be investigated simultaneously. But the combination of (1) knowing the experimental, macroscopic effect of all the imperfections *and* (2) knowing the theoretical, macroscopic effect of individual or a few imperfections, will advance our understanding of which lattice imperfections are present, how they interact with each other, and how they affect the material's response to its environment. This more complete understanding will enable insight into how Pu ages and how its age affects its thermodynamic properties and thermoelastic response.

Approach

(1) Density functional theory (DFT).

The present work considers only the harmonic phonon modes, calculated with density functional perturbation theory as implemented in the VASP package [Kresse1996,Kresse1999]. The electronic states are treated with the projector augmented wave method [Blöchl1994] in the generalized gradient approximation of Perdew, Burke, and Ernzerhof [Perdew1996], with first-order Methfessel-Paxton [Methfessel1989] smearing (width 27 meV), and a cutoff energy for the plane wave basis set of 500 eV. The k-point meshes are chosen for each simulation cell such that their density is at least

40 per $Å^{-1}$. The convergence criteria are 10^{-8} eV for the electronic self-consistency loop and 10^{-7} eV for the ionic relaxation.

(2) Strongly correlated electrons: magnetic structure.

Responsible for Pu's rich phase diagram is the unique dual nature of the *f* electrons: they can be localized or delocalized. DFT is not well equipped to deal with this duality, which reflects a strong correlation between the electrons that is outside the implementation of DFT. Other methods are, in principle, available to address this issue, but they rely on introducing additional parameters and/or are simply too computationally expensive for the purposes at hand.

The approach adopted here relies on using magnetic structure as an approximate treatment of the *f* electrons' strong correlation. Allowing spin polarization in the DFT calculations enables more electrons to occupy spatially different states, effectively keeping the electrons apart. One spin direction's electronic states shift relative to the other spin direction's, broadening the total electronic density of states (DOS), which can lower the total energy similar to crystal-structure distortions.

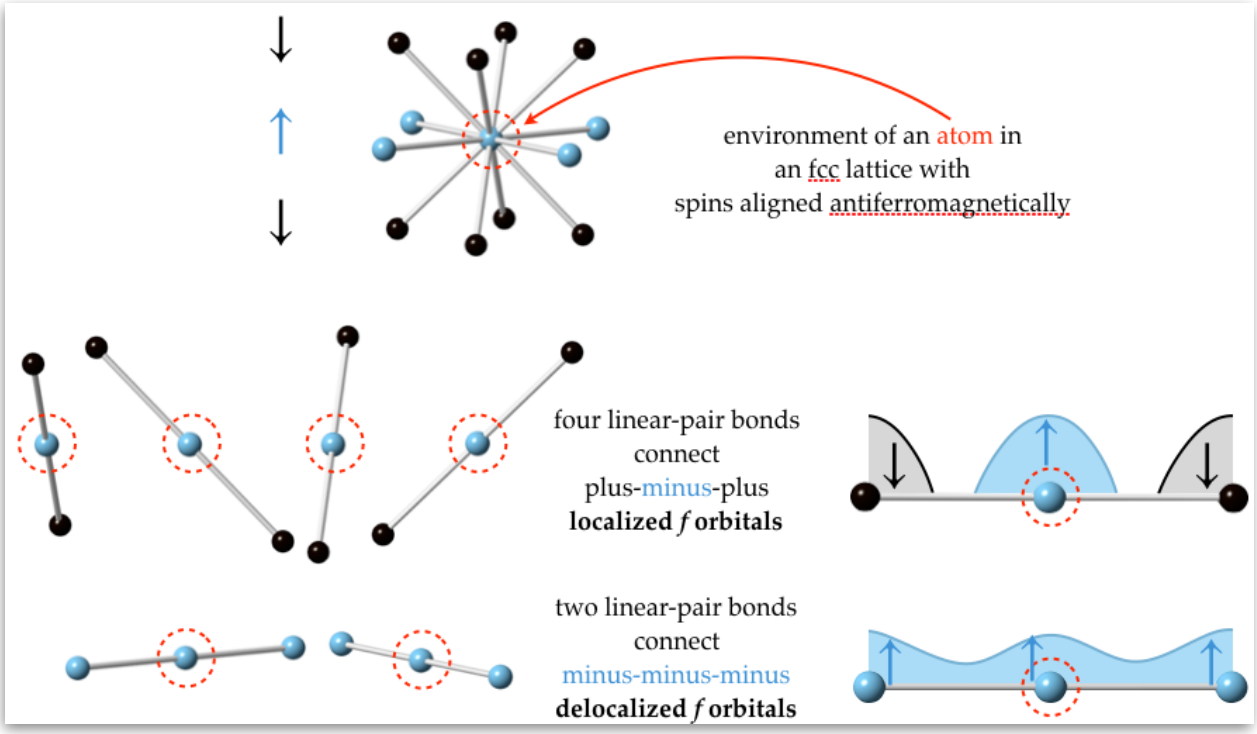

Allowing spin polarization results in a magnetic moment that is not seen in experiment, but the approach does not require any additional parameters and has successfully been used to describe many of Pu's properties, in particular structural details. The phonons of Pu have also been shown to be well described with this approach [Söderlind2019].

(3) Phonons and elastic constants: divide and conquer approach.

The harmonic phonons are calculated with the small-displacement approach [Alfè2001, Alfè2009, Kresse1995]. This involves calculating the forces in response to the displacement of the atoms, followed by post-processing steps that transform the forces into the phonon modes' frequencies and eigenmode patterns. For high-symmetry crystal structures this process can be completed with a small number of DFT calculations. For low-symmetry crystal structures, such as those involving lattice imperfections, the number of DFT calculations becomes much larger, in the worst case six times the number of atoms in the computational cell.

The VASP package has built-in algorithms to perform the needed calculations. However, the calculations are performed sequentially, which (a) does not efficiently use the parallel nature of high-performance computer clusters and (b) becomes untenable for reasonably sized cells (see below) because of wall clock limits. Furthermore, if one of the calculations fails, the entire process fails.

By implementing an array of pre- and post-processing tools based on work by N. Bock, the algorithm has been moved outside of the VASP code. This has enabled the calculations needed for the results described below. The analogous approach for calculating the elastic constants has also been implemented (and given an acronym, CHESTER: CHunked Evaluation of STresses for Elastic Resonse).

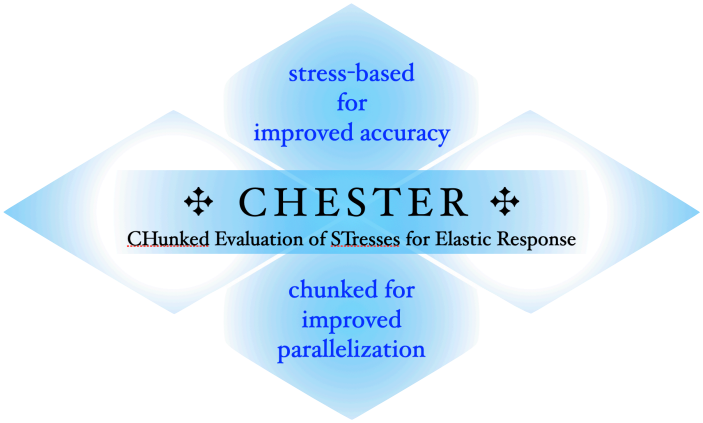

The workflow for both phonon and elastic constant calculations follows the same "divide and conquer" approach (see figure below). With this phonon framework, the largest calculation to date (one interstitial defect added to a 108-Pu atom cell, evaluated at five volumes) required 5x2x328 4-node (144-core) calculations of eleven hours each. All these calculations are independent and could, in principle, be run in parallel as a 472,320-core calculation.

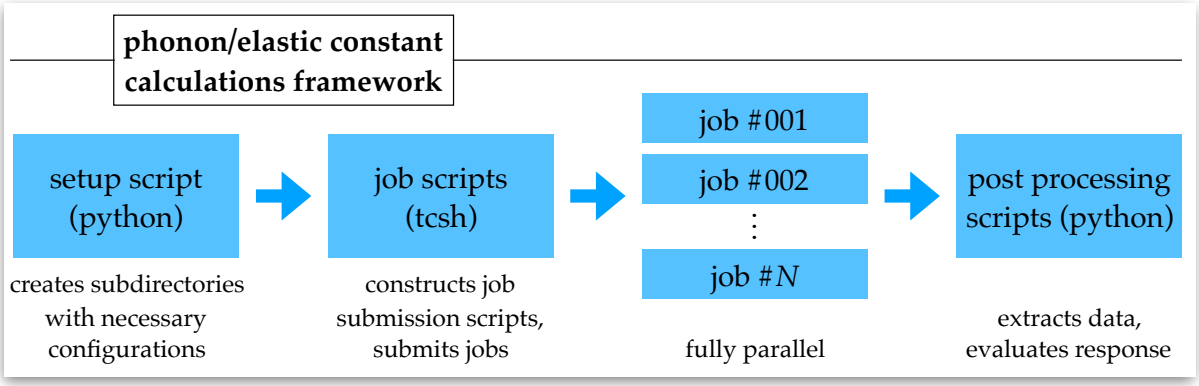

(4) Practical size constraints.

With CHESTER and its phonon equivalent, the size of systems that can be treated are limited by memory and wall clock limits. These limits apply not only to the force calculations, but also to the structural optimization: before the forces can be calculated the system must be structurally optimized. In the case of Pu, this effectively limits the size to a computational cell on the order of those consisting of 3x3x3 conventional fcc cells, with 108 atoms.

While such calculations have been performed for this project, their time to completion hampers the workflow. (The IC cluster snow has a total of 13,248 cores: even complete dedication of it to the phonon calculation outlined above would require a good sixteen days.) In particular, unexpected issues (e.g., the alpha collapse problem, see below) arise and can remain undetected until all the calculations are completed. For these reasons, smaller cells are considered, and the 72-atom cell is chosen as a compromise with which to make progress and establish the processes for possible future expansion. Switching from 108 to 72 atoms, the number of force calculations is reduced by a third and their completion requires about a quarter as long, making progress overall roughly a factor of six faster.

(5) Phonon tracing.

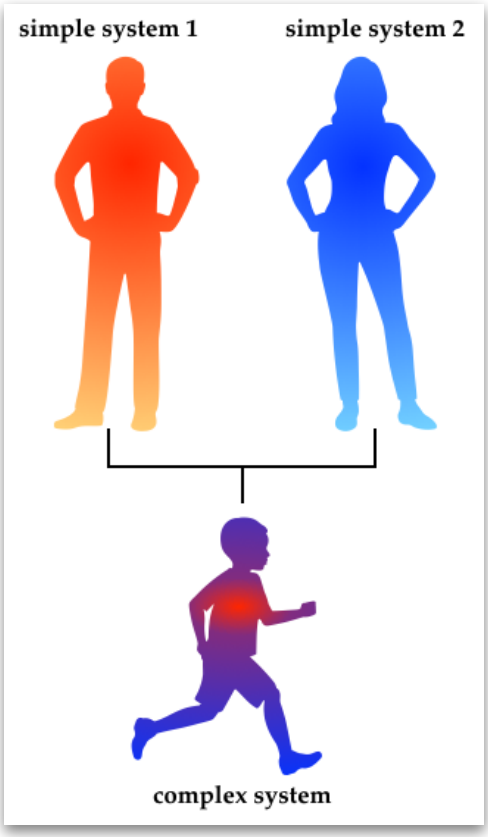

The goal of this project focuses on how the entirety of phonons are affected by lattice imperfections. This provides the thermodynamic insights by evaluating properties that integrate over all the phonon frequencies. However, the details of how lattice imperfections affect individual phonon modes also delivers important information, including (a) how multiple imperfections might interact to change the thermodynamics and (b) how structural phase transformations are driven by imperfection-induced softening (or stiffening) of specific phonon modes.

To understand the effects of lattice imperfections on individual phonon modes, a framework is developed that could loosely be termed “phonon tracing.” The phonon modes are treated like characteristics, which are “inherited” from simpler “parent” systems (e.g., perfect delta-

Pu and an individual Pu atom) by a more complex "child" system (e.g., delta-Pu with a Pu interstitial). The approach also serves to better understand how modes change due to external parameters such as volume.

Results

(1) Alpha collapse.

Pu exhibits six phases that appear at different temperatures. The alpha and the delta phases are the most important, and they are strikingly different in many ways. In particular, Pu undergoes an anomalously large 25% collapse in volume from its largest volume δ phase (δ-Pu) to its low temperature α phase (α-Pu). This is reflected in changes to bond lengths: whereas in δ-Pu's face-centered cubic (fcc) lattice all nearest-neighbor distances are equal (3.3 Å), in α-Pu's monoclinic lattice multiple distances appear, loosely grouped into short (~2.5 Å) and long (~3.1…3.5 Å) bonds.

As shown by Hernandez et al., introduction of an interstitial Pu into a computational δ-Pu cell encourages a local structural phase transition that takes the structure toward an α-Pu like structure in terms of the bonds. This "alpha collapse" appears when the simulation cell volume is slightly decreased.

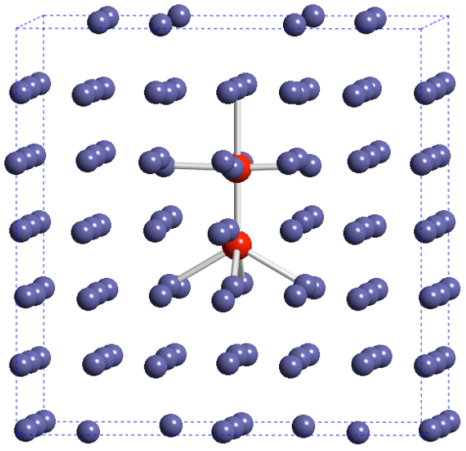

Fig. R1. 108-atom optimized simulation cell with one interstitial Pu atom (upper red sphere) with short bonds drawn as grey cylinders, before alpha collapse. The lattice imperfection is localized and the system's total magnetic moment is low (3.5 μ_B).

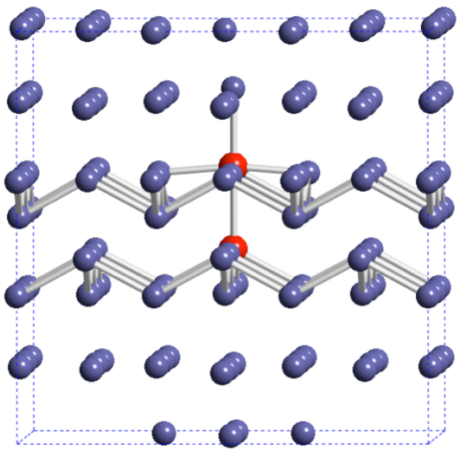

Fig. R2. 108-atom optimized simulation cell with one interstitial Pu atom (upper red) with short bonds drawn as grey cylinders, after the alpha collapse. The lattice imperfection is extended, and the system's total magnetic moment has changed (14 μ_B).

Because a slight decrease in volume leads to the alpha collapse, the calculations fail to give a cold curve with a minimum: the energy jumps down to the other crystal

structure's cold curve. The presence of multiple cold curves suggests modeling Pu with lattice imperfections as multiple phases. However, cold curves representing each of the phases must span both sides of the minimum-energy volume in order to model thermodynamic behavior such as thermal expansion.

(2) Constrained calculations.

To address the alpha collapse problem, computational cells are optimized that are constrained in ways aimed at preventing the alpha collapse. These included Ga substitutions or keeping atoms that are distant from the lattice imperfection in fixed positions relative to one another. To date, one such constrained cell succeeded in avoiding the alphas collapse and is shown in Figs. R3 and R4: a 72-atom cell with the

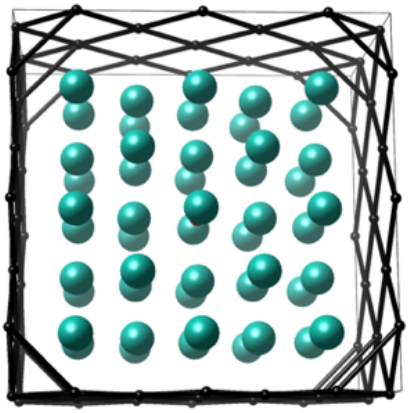

Fig. R3. 72-atom optimized constrained simulation cell: free Pu atoms (teal) inside cage of fixed Pu atoms (black).

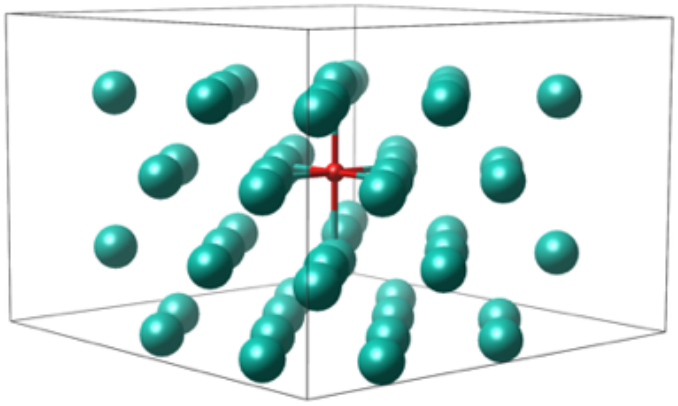

Fig. R4. In the optimized constrained simulation cell, the free Pu atoms show no alpha collapse despite the presence of an interstitial Pu atom (red).

atoms on the box edges held fixed. The computational cells that include Ga substitutions modify the extent of the alpha collapse but do not prevent it entirely.

The logic behind the successful artificial constraint is that the alpha collapse cannot occur at a macroscopic length scale: at some distance from the lattice imperfection, the structure will remain fcc-like. The constrained cell emulates this by forcing the atoms on the box edges to remain fcc-like during the structural optimization.

(3) Constrained 72-atom cell: cold curve, phonons, thermal expansion

Figure R5 shows the cold curve for the successful constrained computational cell. Other cold curves for differently constrained cells are also shown, but these did not prevent the alpha collapse; because of this change in structure their equilibrium volume is smaller (with Ga substitutions contributing further to the change in equilibrium volume).

The optimized structures at each volume serve as starting point to calculate the phonons.

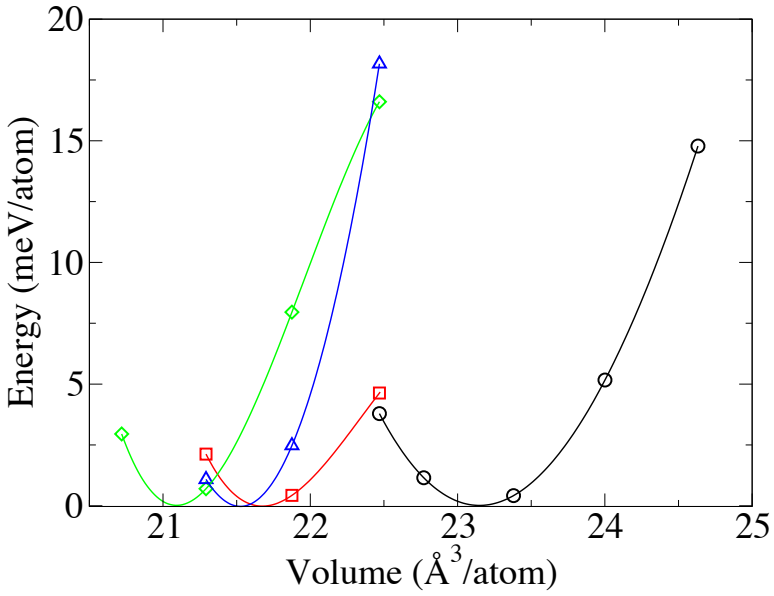

Fig. R5. Cold curves for 72-atom fcc Pu cell with one interstitial Pu and various constraints. The black curve represents results from calculations optimizing the structure within a fixed cage of Pu atoms (see Figs. R3 and R4).

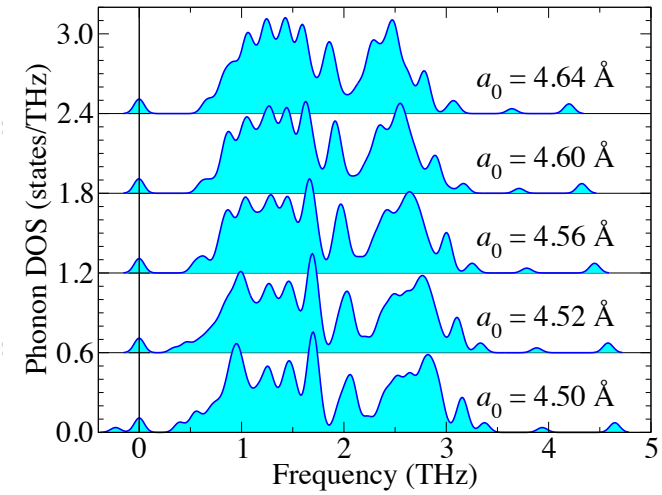

Fig. R6. Calculated phonon densities of states for the cage-constrained 72-atom cell with interstitial. The frequencies of the phonon modes are convoluted with a Gaussian of width σ = 0.05 THz.

The atoms held fixed during structural optimization are *not* constrained for the phonon calculations, and the calculated phonons remain stable even with the constraints lifted, except at the smallest volume (a_0 = 4.50 Å, see Fig. R6), where one mode is unstable. The calculated phonons allow the derivation of a theoretical thermal expansion. At a sequence of temperatures and for each volume, the free energy combines the cold curve energy and the contribution from the phonons. Fitting the free energies for each temperature to a Birch-Murnaghan form delivers the equilibrium volume at that temperature. Figure R7 shows the calculated volumes as a

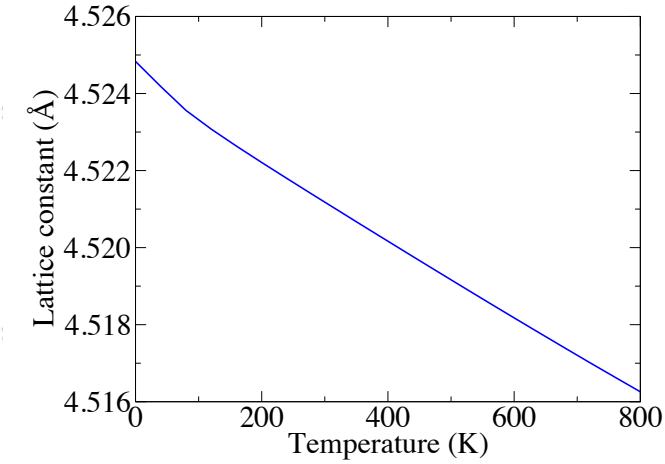

Fig. R7. Calculated thermal expansion for the cage-constrained 72-atom cell with one interstitial Pu.

function of temperature, i.e., the thermal expansion. Unlike the thermal expansion calculated for the perfect delta-phase lattice, here the slope is negative — as it is in experiment [Lawson2006]. This suggests a defect-induced phonon softening causes the experimentally observed negative thermal expansion in δ-Pu.

Phonon "softening" alludes to the frequency of a phonon mode becoming lower with a change in temperature, volume, or other factors such as defect density. The positive thermal expansion observed in most materials stems from a phonon softening with increasing volume: longer bonds generally lower the frequencies of phonon modes, lower frequencies contribute more entropy S to the free energy $F = U - TS$, and increasing the temperature T drives the system toward the state where the phonons are softened.

δ-Pu differs from most materials in that not all phonon frequencies change the same way with changes in volume — even for the perfect fcc lattice. Figure R8 shows that tracing the phonon modes from the experimental lattice constant (4.64 Å) to a smaller value (4.50 Å) reveals that, while the higher-frequency modes tend to stiffen, a large number of low-frequency modes show an unusual softening behavior. In perfect-lattice δ-Pu this softening does not suffice to lead to negative thermal expansion.

This softening of the low-frequency modes is enhanced for the lattice containing an interstitial Pu

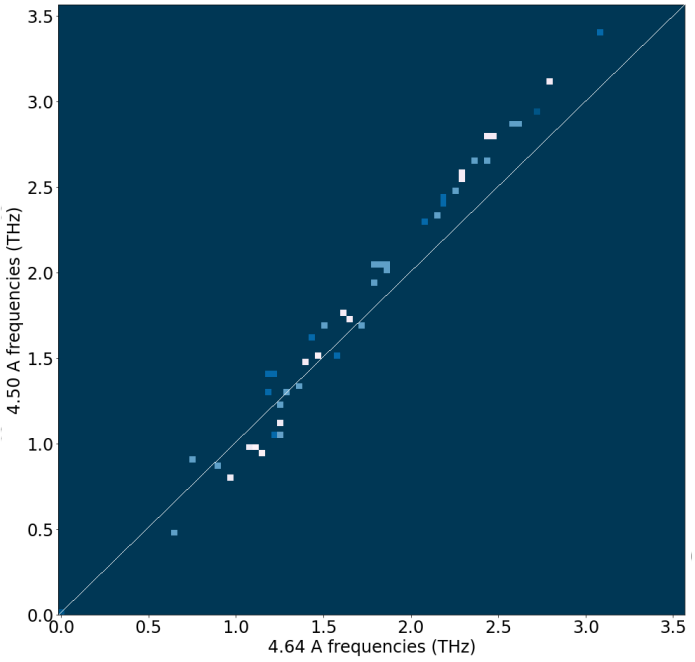

Fig. R8. Calculated phonon mode frequencies for perfect δ-Pu at $a_0 = 4.50$ Å plotted against their frequencies at $a_0 = 4.64$ Å. Unlike most materials, only some frequencies get stiffer (lie above the diagonal line) while others get softer.

atom, which is what drives the thermal expansion to be negative. Figure R9 traces the phonon modes from the experimental lattice constant (4.64 Å) to a smaller value (4.50 Å). Compared to the perfect lattice in Fig. R8, several differences arise. The frequencies appear spread out, as the interstitial lowers the symmetry and thereby removes many degeneracies. Additional high-frequency modes appear due to the introduction of short bonds between the interstitial and the (formerly perfect) fcc lattice. Most notable is the softening of frequencies from just under 1 THz to imaginary values (plotted as negative values).

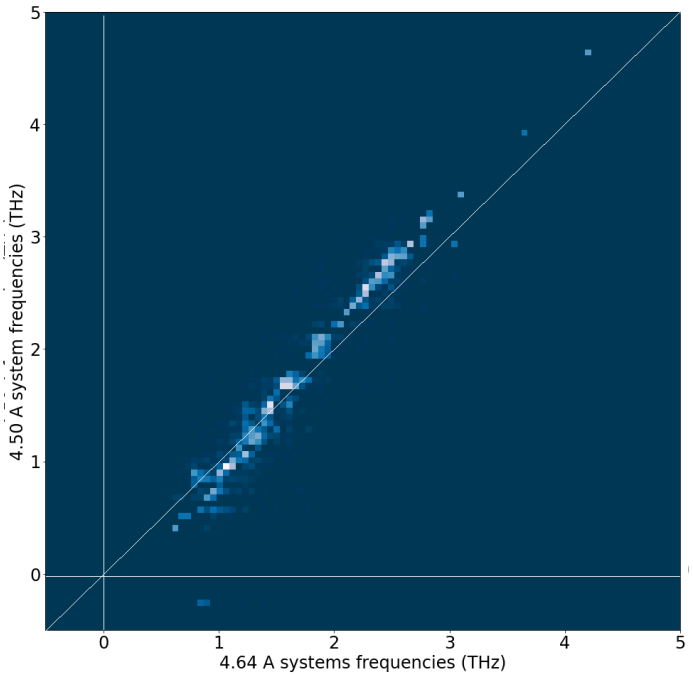

Fig. R9. Calculated phonon mode frequencies for a δ-Pu lattice with an interstitial Pu atom at $a_0 = 4.50$ Å plotted against their frequencies at $a_0 = 4.64$ Å.

a_0	Frequency
4.64 Å	0.83 THz and 0.93 THz
4.60 Å	0.76 THz
4.56 Å	0.62 THz
4.52 Å	0.34 THz
4.50 Å	0.23*i* THz (unstable)

These modes describe the pattern of atomic movement that is the alpha collapse, indicating that at $a_0 = 4.50$ Å the system would lower its energy by following that pattern. At larger lattice constants, the frequencies of the modes are positive, i.e., the modes are stable, but the modes soften considerably before becoming unstable, as shown in the table at left.

Based on the thermal expansion, the volume for the system is given as a function of temperature. Once elastic constants have been calculated at the different volumes, these can be combined with the temperature dependence of the volume to evaluate the temperature dependence of the elastic constants. Similarly, the heat capacity evaluated from the calculated phonons at each volume can be combined with the temperature dependence of the volume to provide the heat capacity as a function of temperature.

Summary

The work described here shows a path forward toward a first-principles based understanding of how lattice imperfections affect the thermodynamics of Pu. The outlined workflow consists of

1. using a computational cell that is large enough to show the relevant physics yet small enough for the calculations to be feasible in a reasonable amount of time,
2. imposing constraints on the computational cell such that relevant crystal structures can be optimized above and below their (theoretical) equilibrium volume for the calculation of a cold curve,
3. applying a chunking of the individual calculations needed to evaluate the phonons and elastic constants, from which the physical observables (thermal expansion, heat capacity, elastic moduli) are calculated for comparison with experiment, and
4. studying the resulting phonon modes with the newly-developed phonon tracing approach for a deeper understanding at the atomistic level.

This workflow is followed (with the exception of the elastic constants) for a 72-atom δ-Pu computational cell with an interstitial Pu atom. The atoms on four edges of the cell are constrained during the optimization, but no longer held fixed for the calculations of phonons. The evaluated thermal expansion is negative, as measured experimentally, and an atomic-level understanding is provided.

Onward to other lattice imperfections and comparison with experiment!

Acknowledgements

Funding is generously provided by Campaign 2 and the Equation of State Project under the Physics and Engineering Models Program of the Advanced Simulation and Computing Program.

Significant gratitude is expressed to Scott Crockett, Anthony Fredenburg, Franz Freibert, Sarah Hernandez, and John Wills for numerous insightful and encouraging scientific discussions, as well as to Scot Halverson for critical computational assistance and to Manolo Sherrill for critical computational support.

References

[Alfè2001] D. Alfè, G. D. Price, and M. J. Gillan, Phys. Rev. B 64, 045123 (2001).

[Alfè2009] D. Alfè, Computer Physics Communications 180, 2622 (2009).

[Blöchl1994] P. E. Blöchl, Phys. Rev. B 50, 17953 (1994).

[[Kresse1995] G. Kresse, J. Furthmüller, and J. Hafner, Europhysics Letters 32, 729 (1995).

Kresse1996] G. Kresse and J. Furthmuller, Phys. Rev. B 54, 11169 (1996).

[Kresse1999] G. Kresse and D. Joubert, Phys. Rev. B 59, 1758 (1999).

[Lawson2006] A. C. Lawson , J. A. Roberts , B. Martinez , M. Ramos , G. Kotliar , F. W. Trouw , M. R. Fitzsimmons , M. P. Hehlen , J. C. Lashley , H. Ledbetter , R. J. Mcqueeney, and A. Migliori, Invar model for delta-phase Pu: thermal expansion, elastic and magnetic properties. Philosophical Magazine 86, 2713 (2006).

[Lindsay2019] L. Lindsay, A. Katre, A. Cepellotti, and N. Mingo, Journal of Applied Physics 126, 050902 (2019).

[Methfessel1989] M. Methfessel and A. T. Paxton, Phys. Rev. B 40, 3616 (1989).

[Perdew1996] J. P. Perdew, K. Burke, and M. Ernzerhof, Phys. Rev. Lett. 77, 3865 (1996).

[Söderlind2019] P. Söderlind, A. Landa, and B. Sadigh, Advances in Physics 68, 1 (2019).